

# Chirality communications between inorganic and organic compounds

Bing Ni  | Helmut Cölfen 

Physical Chemistry, Department of Chemistry, University of Konstanz, Konstanz, Germany

## Correspondence

Bing Ni and Helmut Cölfen, Physical Chemistry, Department of Chemistry, University of Konstanz, Universitätsstrasse 10, D-78457 Konstanz, Germany.

Email: [bing.ni@uni-konstanz.de](mailto:bing.ni@uni-konstanz.de) and [helmut.colfen@uni-konstanz.de](mailto:helmut.colfen@uni-konstanz.de)

## 1 | INTRODUCTION

Chirality spans over almost every size range, from molecules to biological systems and even to galaxies. It is one of the fascinating geometrical properties with a lot of amazing manifestations in the material world. As chemical researchers, we are more interested in chirality at the molecular scale and nanoscale. Chiral molecules are found important in life science, agrochemicals, pharmaceutical industries, biosensing, display materials, and so forth.<sup>1–5</sup> Chirality stems from a structure lacking symmetry elements of inversion symmetry and mirror-plane, which makes the structure not superimposable with its mirror image. Without these two kinds of symmetries, any structure is chiral, besides conventional chiral organics or spiral inorganic structures. The essence of chirality is the stereochemistry of molecules or nanostructures.

The history of stereochemistry can trace back to the discrimination of tartaric acid enantiomer crystals, which was made by Louis Pasteur in 1848.<sup>6</sup> He concluded that the optical activity of organic compounds arose from a lack of symmetry of the molecules and crystals from the dissymmetric packing of nondissymmetric molecules.<sup>7</sup> The stereochemistry of organics has been burgeoning since then. To date, optical activity is still a major method to analyze chiral molecules and chiral nanostructures. In fact, optical rotation behavior was first observed within inorganic materials: Quartz crystals by Jean-Baptiste Biot in 1812.<sup>7,8</sup> However, the stereochemistry of inorganics has remained largely unexplored as compared to organics. One of the reasons might be that even a single

chiral inorganic nanoparticle (NP) is a complex system whose optical activity is caused by several factors simultaneously, let alone the ensemble of NPs, which is the common form of the researched NPs. Now with the tremendous advancement in preparing monodispersed NPs, as well as the deeper understanding of the interaction of light with matter, the field of chiral inorganic materials is actively growing.

In nature, there are many organic–inorganic hybrid chiral structures, such as the shell of snails, crab carapace, and so forth. The formation of the inorganic parts in these materials is generally guided by the chiral organic compounds, and the organics impart the chirality of the hybrid materials.<sup>9</sup> More interestingly, *Nature* showed homochirality in that the amino acids in organisms are L-type, though sugars are D-type. L-type means the compounds could rotate the plane of linearly polarized (LP) light in a left-handed or counterclockwise fashion, whereas D-type in a right-handed or clockwise fashion. The origin of homochirality is one of the 125 most compelling questions raised by *Science* magazine.<sup>10</sup> One of the promising answers is that inorganic materials, which obtain chirality from external fields, endow bioorganic compounds with homochirality.<sup>11</sup>

Chirality can be transferred from one compound to another at suitable conditions. The 2001 Nobel Prize of chemistry was awarded to chirally catalyzed hydrogenation and oxidation reactions. These works demonstrated the synthesis of enantiopure organic compounds by asymmetric catalysis. The process can be seen as amplifying chirality or transferring chirality from catalysts

This is an open access article under the terms of the Creative Commons Attribution License, which permits use, distribution and reproduction in any medium, provided the original work is properly cited.

© 2021 The Authors. *SmartMat* published by Tianjin University and John Wiley & Sons Australia, Ltd.

(usually metal complexes) to organic compounds. The opposite transfer is also possible. Chiral organics can help synthesize chiral-shaped inorganics or serve as a template or matrix to provide chiral environments around inorganics, which all lead to chirality in inorganics.

Chirality recognition is another type of communication. Such recognition is vital in biosystems. For example, humans can only digest D-sugars but not L-sugars because the enzymes cannot bind with L-sugars. Chirality recognition has been widely researched in supramolecular chemistry.<sup>12</sup> The assembling or crystallization of one enantiomer would repel another enantiomer in some cases, leading to homochiral ensembles.<sup>13,14</sup> Or a trace amount of chiral molecules induces the homochiral assembling of another type of molecules.<sup>15–17</sup> More recently, chiral porous materials, such as metal-organic frameworks (MOFs), covalent organic frameworks (COFs), and so forth, have been developed to recognize and separate enantiomers.<sup>18,19</sup> The chiral MOFs and COFs can also serve as asymmetric catalysts due to their different binding strength with substrates or intermediates.<sup>20,21</sup>

The chirality communications mainly include transfer and recognition. These communications have been widely discussed in organic compounds, leading to the flourishing of stereochemistry and supramolecular chemistry of organics. Although the library of organics is large, there are even more inorganic species, and inorganics have many unique properties. The fundamental facts of the chirality communications are the matching and packing of atoms or molecules. Thus, there are lots of exciting aspects and potential in studying communications between inorganic and organic compounds. For organics, such communications could help to develop new potential methodologies of asymmetric synthesis, smart material systems, novel physical–chemical properties, and so forth, which might be found in inorganics. More opportunities could be expected with the development of this field. In this report, we would like to focus on the communications between inorganic and organic compounds. We would start with a brief discussion on the features of chiral organic and inorganic compounds. Then we would move to the chirality transfer from organics to inorganics and the recognition of enantiomers on chiral inorganic structures. At last, we would outlook some unexplored topics, as well as discussing the difficulties in this field.

## 2 | FEATURES OF CHIRAL COMPOUNDS

As we have mentioned before, chirality stems from the lacking of inversion symmetry and mirror-plane in the structures. The chiral forms in organics and inorganics

are different (Figure 1). In organic materials, most of the chirality is an inherent feature of covalent C bonds. The  $sp^3C$  center makes the structure a tetrahedron configuration. When the four connecting elements or groups around the C center are all different, inversion symmetry and mirror-plane are missing. Consequently, chirality would evolve (Figure 1A). For example,  $CHClBrI$  is chiral. The chirality in molecules could transfer to larger and more complicated systems. Biosystems inherit the chiral features of the organic compounds. The stereochemistry of small molecules could influence the packing and folding of the supramolecular systems, such as DNA, peptides, proteins, and so forth. Steric hindrance can also lead to chiral structures, such as spirotype conjugated systems like spiropyran, helicene, chiral supramolecules, and so forth.

The chirality in inorganic materials is more complicated. The inorganic stereochemistry should consider all the lattice structure, surface structure, and environment of the particle. We may have feelings that chiral inorganic materials are rare. That is because inorganic NPs are very likely to be racemic, and they are extremely difficult to separate. Most irregular-shaped particles are chiral according to the symmetry. These kinds of asymmetric structures are one type of chiral inorganics (Figure 1C1). Furthermore, many crystals are inherently chiral according to their symmetry of the crystalline lattice. There are 65 space groups that feature chirality (Figure 1B). Any lattices belonging to these space groups are chiral. Quartz crystal is a typical example (Figure 1C2). The shape of these crystals would also replicate the symmetry of the lattice, providing a possible way to manually purify the enantiomers. However, the chiral resolution becomes much more difficult or even impossible when the size of the crystals is small. There is another kind of chirality in inorganic materials called surface chirality.<sup>3</sup> In fcc metals, high-index facets with Miller indices of  $h \neq k \neq l \neq k$  and  $h \times k \times l \neq 0$  are chiral.<sup>23</sup> Such high-index facets can be seen as the combination of (111), (110), and (100) terraces, and the arrangement of these terraces can be used to determine the handedness of the surface (Figure 1C3). These three forms can guarantee the chiral inorganic entities. On the contrary, achiral inorganic particles can be endowed with chirality by assembling them in a chiral way or adsorbing chiral organic molecules<sup>24–26</sup> (Figure 1C4,C5).

The synthesis of chiral organic compounds largely relies on asymmetric catalysis, which can provide a controllable and powerful method to prepare enantiopure compounds. Chiral templates can also be employed to prepare chiral supramolecules. For example, high-speed stirring would induce vortex in a solution, which offers a good template to prepare spiral assembling

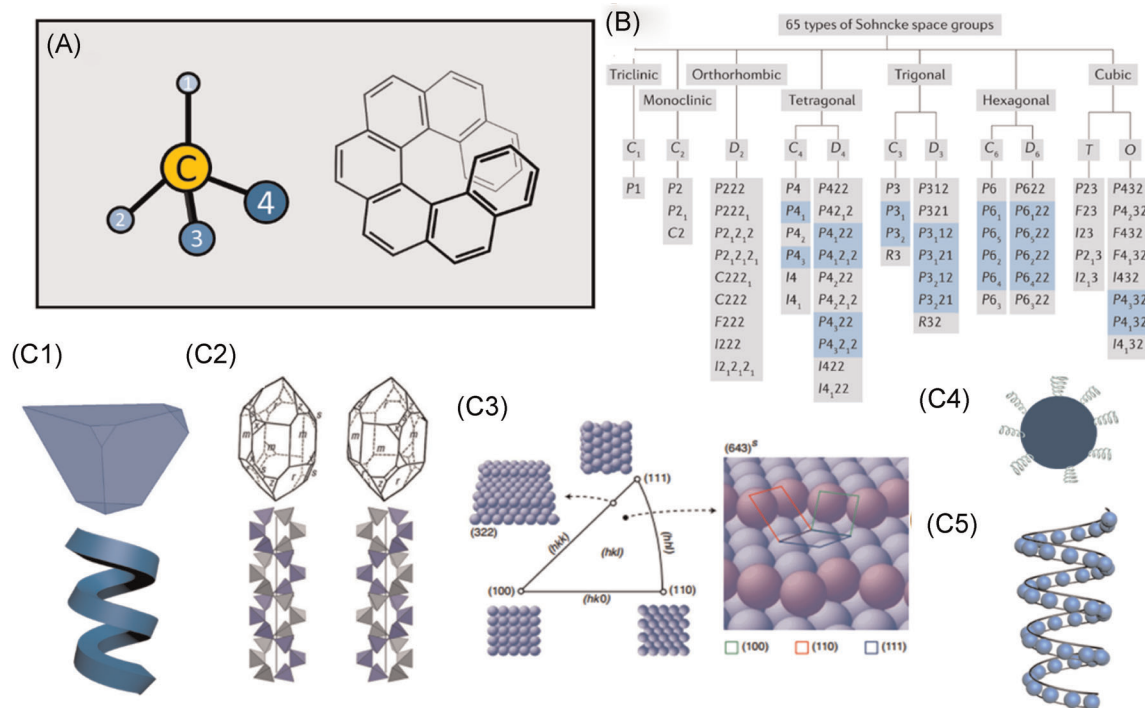


**FIGURE 1** (A) Chiral forms of organics. (B) Chiral space groups are highlighted in blue, any lattice belonging to the 65 listed Sohncke space groups are chiral. Adapted with permission.<sup>22</sup> Copyright 2020, Springer Nature. (C) Chiral forms of inorganics. (C1) asymmetric shapes; (C2) crystals of chiral lattice, the lattices here show enantiomorphic  $\alpha$ -quartz crystal and corresponding crystal structure. Adapted with permission.<sup>5</sup> Copyright 2019, Wiley-VCH. (C3) Chiral surface of fcc metals. Adapted with permission.<sup>3</sup> Copyright 2020, Springer Nature. (C4) Individual nanoparticle (NP) encapsulated by chiral organics; (C5) achiral NPs arranged in a chiral way or embedded in the chiral matrix

structures.<sup>27,28</sup> When the interactions between monomers are strong enough, the spiral structure can be maintained even if the stirring is stopped.<sup>29</sup> This method can also be used for inorganics. For example, MoS<sub>2</sub> nanosheets and carbon nanotubes have been assembled to spiral structures with high-speed stirring with the help of P123 polymers.<sup>30</sup> External fields have been widely used to prepare chiral inorganics. They are very controllable in some situations. For materials that interact strongly with light, such as plasmonic metals and semiconductors, circularly polarized light (CPL) is a potential tool to induce chirality. In a straightforward system, Au synthesis under the illumination of CPL could end up with chiral Au NPs.<sup>31</sup> This method was also available to assemble CdTe NPs to twisted nanoribbons in a controlled manner.<sup>32</sup> Mechanical or magnetic fields can be used to transfer macroscale asymmetry to the nanoscale as well.<sup>33,34</sup> In chiral inorganic material synthesis to date, the external fields are usually more controllable than simple growth methods. The growth methods heavily depend on the existence of chiral molecules as modulators in the growth process. However, no simple rules have been summarized yet and the works are still in the trial-and-error mode.

As the synthesis favors racemic products, the chiral resolution is very vital to obtain enantiopure products. For organics, crystallization of one enantiomer is a crucial method to purify the products. However, only a small group of racemates could crystallize in an enantiopure way; others stay at the racemic form even in crystals or called conglomerate crystallization.<sup>35</sup> It is revealed that strongly heterogeneous interactions across the molecules, which depend on molecules' inherent structures, would favor the spontaneous resolution of racemic mixtures in the crystallization process.<sup>36</sup> Indeed, it has been demonstrated that chiral double-hydrophilic block copolymers could separate a racemic calcium tartrate hexahydrate mixture by slowing down the crystallization of the thermodynamically most stable racemic mixture as well as one of the enantiomers to kinetically control the crystallization of the other enantiomer, thus separating the racemic mixture.<sup>37</sup>

Alternatively, chromatographic separation and membrane-assisted separation are more used in applications for the resolution, but the yields are small with current technology. Alternatively, density gradient ultracentrifugation has been demonstrated to separate racemic DL-alanine from enantiomer crystals due to very

small differences in the particle density of the racemate and enantiomer crystals.<sup>38</sup> With good recovery rates of 70%–90% and the possibility of upscaling to preparative or even industrial crystallization, this is an interesting separation method following kinetic enrichment of one enantiomer in a racemic mixture by crystallization. On the contrary, there seems to be no effective method to separate chiral inorganic NPs.

The chirality of organics is encoded in covalent bonds, which are possible to be manipulated. Judiciously designing photoresponsive C=C bonds or N=N bonds in the molecules can impart the compounds with controllable responsive behavior.<sup>39</sup> Protons and metal cations are also found possible to induce switchable chiroptical properties.<sup>40,41</sup> This behavior offers a new dimension for the design of molecular switches, as well as other smart matter systems operating at molecular levels. The organic-inorganic hybrid systems can exhibit the responsiveness of the organics, such as the Au-DNA systems.<sup>42–44</sup> On the contrary, the chemical bonds in inorganics are less versatile than those in organics. The responsive behavior in inorganic systems requires more complicated designs. Morisawa et al.<sup>45</sup> designed an interesting Au nanorod supported on the TiO<sub>2</sub> system to realize the responsiveness. They illuminated circularly polarized light (CPL) on the system to deposit PbO<sub>2</sub>

around Au, and the chirality was encoded in the PbO<sub>2</sub>-Au-TiO<sub>2</sub> structures. On the other hand, the PbO<sub>2</sub> could be degraded by UV-induced TiO<sub>2</sub> catalysis, and the chirality was also eliminated. Such response was reversible and repeatable. The chiroptical response could also be realized by coupling the chiroptical properties with other physical properties. For example, Zhuang et al.<sup>46</sup> judiciously designed a Zn<sub>x</sub>Cd<sub>1-x</sub>S-Ag<sub>2</sub>S/Au@Fe<sub>3</sub>O<sub>4</sub> system, which couples the chiroptical properties with magnetic properties. The dissymmetry factor (g-factor) could be reversed and enhanced by 70 times when a magnetic field was applied.<sup>46</sup> Such enhancement was attributed to the local magnetic field induced by the Fe<sub>3</sub>O<sub>4</sub> domain under an external magnetic field. The local magnetic field changed the electric transition dipole moment of the hybrid material, leading to different adsorption of left-handed and right-handed CPL. Accordingly, the chiroptical property was changed.

A comparison between chiral organics and inorganics is shown in Table 1. Moreover, the physical and chemical properties of inorganics are very different from those of the organics; thus it is highly demanding to develop novel inorganic chiral systems.<sup>1</sup> The interaction of light could be much stronger in inorganics, which could lead to significantly higher dissymmetry factors.<sup>47</sup> Such high dissymmetry factors, together with nanotechnology, are

**TABLE 1** A comparison between chiral organics and inorganics

	Organics	Inorganics
Chiral form	Asymmetric sp <sup>3</sup> carbon Steric hindrance-induced asymmetry	Chiral surface, chiral shape Chiral lattice Nanoparticles (NPs) in chiral matrix Asymmetric packing of NPs
Preparation	Asymmetric catalysis Chiral-templated assembling	Chiral-templated assembling Chiral external field-induced growth or assembling Chiral organics modulated growth
Chiral resolution	Enantiopure crystallization Chromatographic separation Membrane-assisted separation	Manual discrimination of visible crystals
Responsiveness	Triggered by light, pH, ions, and so forth. Usually accompanied with carbon backbone change	Complicated designs of the structures and properties of the system Could be coupled with the magnetic field and other properties Inorganic-organic hybrid systems could inherit the properties of organics
Applications	Life science; agrochemicals; pharmaceutical industries; bio-sensing; display materials	Biosensing; display materials; chiral catalysis; chiral resolution; biomedical imaging; information technologies; smart systems

promising in new technological solutions in many fields, such as biosensing, chiral catalysis, chiral resolution, biomedical imaging, information technologies like quantum computing, and so forth.<sup>1</sup> Coupling chiroptical properties with other physical properties would be easy due to the virtue of inorganics, which could offer new perspectives on material science as well. Moreover, a deeper understanding of the inorganic chirality can not only shed light on possible answers to the homochirality on Earth but also help to design complicated biomimetic chiral technologies. To realize these advantages, developing robust, reproducible, and low-cost methods to prepare enantiopure inorganics is the first step.

### 3 | CHIRALITY COMMUNICATIONS BETWEEN ORGANIC AND INORGANIC COMPOUNDS

The explored chiral inorganics span over clusters, noble metals, semiconductors, metal oxides, MOFs, and so forth. The currently most investigated communications are their synthesis with the help of chiral organics and the enantioselective adsorption of organics on their surfaces. A summary is presented in Figure 2.

#### 3.1 | Chirality transfer from organics to inorganics

Some of the inorganics contain chiral ligands as compositions, thus, the chirality is directly transferred from organics to inorganics. Others contain no chiral ligands; thus, the transfer should be achieved in other indirect ways.

The direct way contains two types: chiral organics in the lattice or on the surface. Some hot material groups of

the “in lattice” type are the hybrid organic–inorganic perovskites (HOIPs),<sup>22</sup> zeolites, MOFs, so forth. It is worth mentioning that the HOIPs do not necessarily have a perovskite  $ABO_3$  form. Their structures are quite tunable, as well as their energy bands. HOIPs have arisen significant interests in material science. Normal perovskites belong to the  $Pm3m$  space group, which is symmetric. When chiral organics are introduced into the system, the symmetry would be greatly decreased to the noncentrosymmetric type. Such symmetry would endow materials with additional functions like chirality or chiral responsiveness. Some representative applications of chiral HOIPs are shown in Figure 3. The first chiral HOIP was reported in 2003 by Billing and Lemmerner,<sup>48</sup> but this topic became hot only recently. Ahn et al.<sup>49</sup> employed S- and R-methylbenzylamine (MBA) into the HOIPs and first explored the chiroptical behavior in 2017. Later they found that the chiroptical properties can be readily tuned by compositions according to their excitonic band structures and crystal-structure changes.<sup>50</sup> The chirality can be imparted on the electronic structure of the semiconductors and brings about circular polarization of photoluminescence,<sup>51</sup> or highly sensitive CPL detections.<sup>52</sup> Furthermore, spin-polarized photon adsorption and spin-polarized photoluminescence can be tuned by composition change or a magnetic field.<sup>53</sup> The spin of charge could be modulated as well. The perovskite  $(MBA)_2Pb_{1-x}Sn_xI_4$  films, including R/S-MBA, showed a spin-polarization in the current-voltage characteristics as high as 94%, arising from the chiral-induced spin selectivity effect.<sup>54</sup> Thanks to the nonsymmetric space group, ferroelectricity has been demonstrated in a 2D [R- or S-1-(4-chlorophenyl) ethylammonium]<sub>2</sub>PbI<sub>4</sub> materials.<sup>55</sup> A strong second-harmonic generation response has been found in chiral HOIPs as well.<sup>56,57</sup> More investigations are ongoing now.

Zeolites and MOFs represent materials with accessible hollow interiors. When homochiral environments are

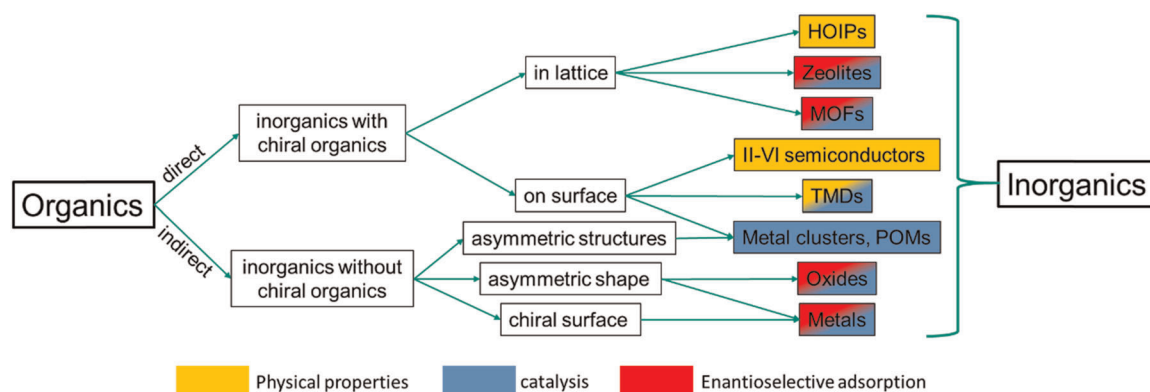


FIGURE 2 Summary of the direct and indirect chirality transfer from organics to inorganics. The highlighted colors mark the currently investigated applications of the corresponding chiral materials

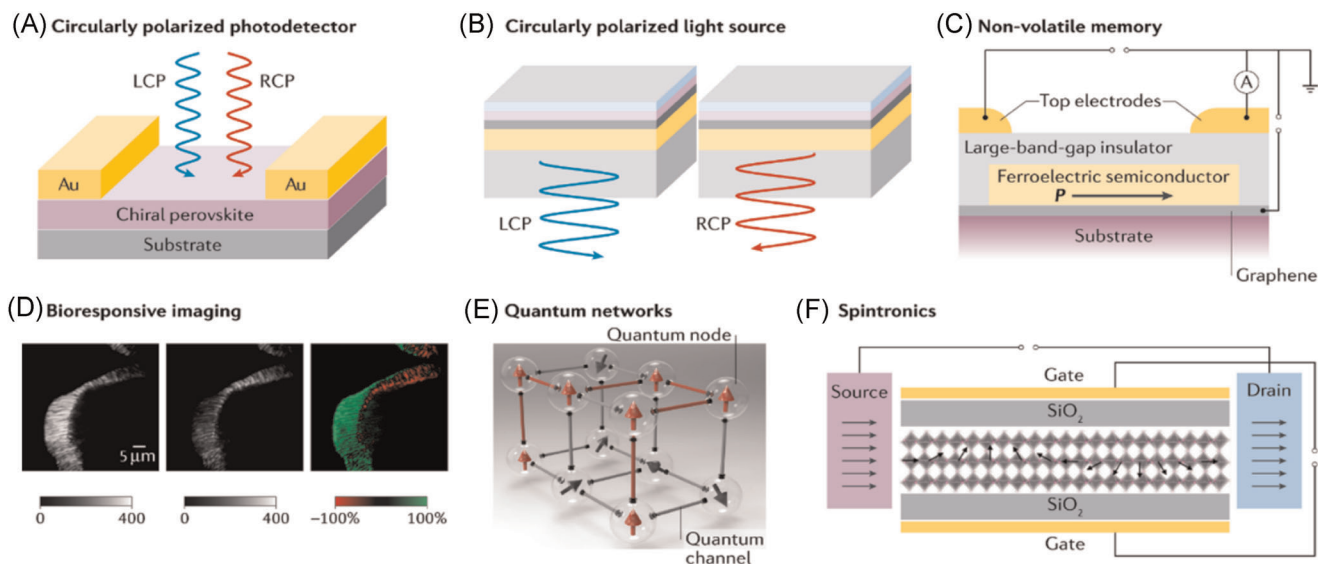


FIGURE 3 Some representative applications of the hybrid organic–inorganic perovskites. Adapted with permission.<sup>22</sup> Copyright 2020, Springer Nature

implanted in the pores, enantioselective separation and catalysis can be rationally obtained. For example, Seo et al.<sup>58</sup> developed a robust chiral zeolite named D- or L-POST-1, and realized the chiral resolution of racemic  $[\text{Ru}(2,2'\text{-bipy})_3]\text{Cl}_2$  (bipy = bipyridine) by enantioselective adsorption. Asymmetric transesterification reactions were also found.<sup>58</sup> In another example, different isostructural chiral MOFs based on MOF-1 were used in the asymmetric transfer hydrogenation of heteroaromatic imines (benzoxazines and quinolines), and an enantioselectivity up to 97% has been achieved.<sup>59</sup> Due to their excellent structural diversity, many different chiral porous materials were developed and used in the chiral resolution of racemic organics.<sup>18</sup>

The interest in preparing chiral NPs by immobilizing chiral organics on achiral cores could be traced back to the early 2000s. In 2007, Moloney et al.<sup>60</sup> first reported the chiroptical properties of D- or L-penicillamine capped CdS NPs. Such achiral semiconductor@chiral-ligand structures combined the features of optically active organics and luminescent NPs, which resulted in circularly polarized luminescence. As the luminescence properties heavily rely on the size and shape of the semiconductors, much attention has been paid to the synthesis, morphology control, and composition control of the achiral cores.<sup>61</sup>

There are two general strategies to obtain the “on-surface” chirality. One is the direct synthesis of NPs with chiral ligands as capping agents. In this method, cysteine, glutathione, and penicillamine are the most used ligands. The other method is the postmodification of NPs with chiral molecules, such as exchanging the original surface ligands with chiral molecules or supramolecular co-assembly of NPs with chiral gelators.<sup>62</sup> The optical activity of these materials

has been widely studied through theoretical models using discrete dipole approximation,<sup>63</sup> time-dependent density functional theory,<sup>64</sup> density functional theory, and ab initio molecular dynamics,<sup>65</sup> or nondegenerate coupled-oscillator models.<sup>66</sup> As the method to control the optical properties of semiconductor NPs has become mature now, the circularly polarized luminescent properties of such achiral-NPs@chiral-organics are very controllable and tunable. Furthermore, this kind of transfer process has also been validated in transition metal dichalcogenides.<sup>67</sup>

Downsizing NPs leads to clusters. Achiral-cluster@chiral-ligand configurations are also common in noble metal clusters. Schaaff et al.<sup>68</sup> report an Au@glutathione structure as early as 1998. Chiral Au clusters have attracted broad research interests due to their potential in both fundamental science and application.<sup>69,70</sup> The achiral-core@chiral-ligand configuration is just one kind of the chiral clusters, such as  $\text{Au}_{246}(\text{SR})_{80}$ , where R is 4-methylbenzenethiol ligands (Figure 4A).<sup>71</sup> There are two more kinds of chiral clusters: (1) chiral metal kernels, such as  $\text{Au}_{20}(\text{SR})_{16}$ <sup>72</sup> (Figure 4B); (2) chiral arrangement of staple motifs on the surface, such as  $\text{Au}_{38}(\text{SR})_{24}$ <sup>73</sup> (Figure 4C). In these clusters, chiral organics are not employed in the synthesis and final structures. The chirality originates from the stereochemistry of the Au and ligand packing.<sup>74</sup> Thus, the obtained products are usually racemic. Dolamic et al.<sup>75</sup> found that high-performance liquid chromatography could be used to separate different enantiomers. But such a method has not been widely employed in the resolution of chiral clusters yet. Similar kinds of chiral forms could also be found in polyoxometalates.<sup>76</sup>

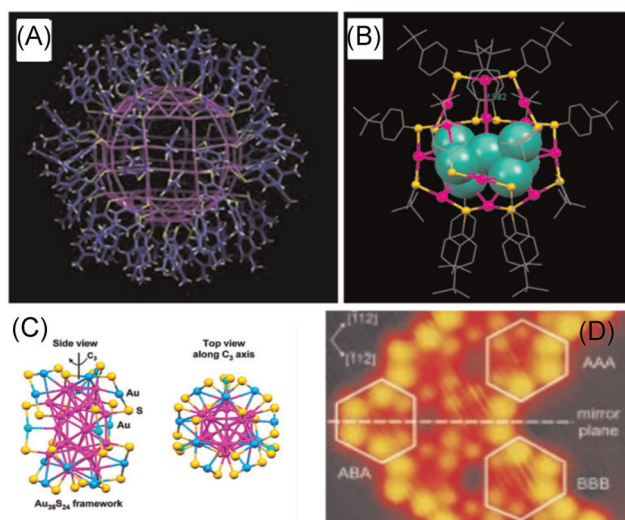


**FIGURE 4** Chiral clusters and chiral surface. (A)  $\text{Au}_{246}(\text{SR})_{80}$ , in which the chirality is imparted by the whirls of carbon tails in the ligand assembly. Adapted with permission.<sup>71</sup> Copyright 2016, AAAS. (B)  $\text{Au}_{20}(\text{SR})_{16}$  with the Au7 chiral kernel shown in the space-filling form. Adapted with permission.<sup>72</sup> Copyright 2014, ACS. (C)  $\text{Au}_{38}(\text{SR})_{24}$  with the chiral arrangement of staple motifs. Adapted with permission.<sup>73</sup> Copyright 2010, ACS. (D) Scanning tunneling microscopy image of the HtBDC leached Cu(110) surface. Hexagonal AAA and BBB areas are chiral, whereas the ABA area is racemic. Adapted with permission.<sup>77</sup> Copyright 2001, Wiley-VCH

When ligands adsorb on some surface, the surface structure might be reconstructed in some cases. Chirality is possible to be imprinted on the surface accordingly. Schunack et al.<sup>77</sup> studied the chiral twisting hexa-tert-butyl-decacyclene (HtBDC) molecules adsorbing on the Cu(110) surface. When they used a scanning tunneling microscopy tip to move the HtBDC molecules away from their preferred adsorption sites, atomic-scale divots or trenches could be created on the Cu(110) surface as the HtBDC would extract some Cu atoms out. Such trenches were visibly chiral and the handedness was determined by the chirality of the HtBDC structures<sup>77,78</sup> (Figure 4D). This kind of imprinting process could also be validated by using L-lysine as the chiral ligand.<sup>79</sup> In most of the reported results, the chiral organics remained on the surface. However, the surface after the imprinting process was intrinsically chiral. The remaining organics might hinder the further utilization of such surfaces. If the bare chiral surface could be obtained, such a transfer process could be seen as an “indirect transfer.”

A typical “indirect transfer” process is the synthesis of highly optical active nanomaterials in the presence of chiral ligands, and the chiral ligands are removed after synthesis. González-Rubio et al.<sup>80</sup> reported the successful synthesis of chiral Au nanorods with spiral wrinkles by guiding the Au atom diffusion direction through chiral micelles (Figure 5A).

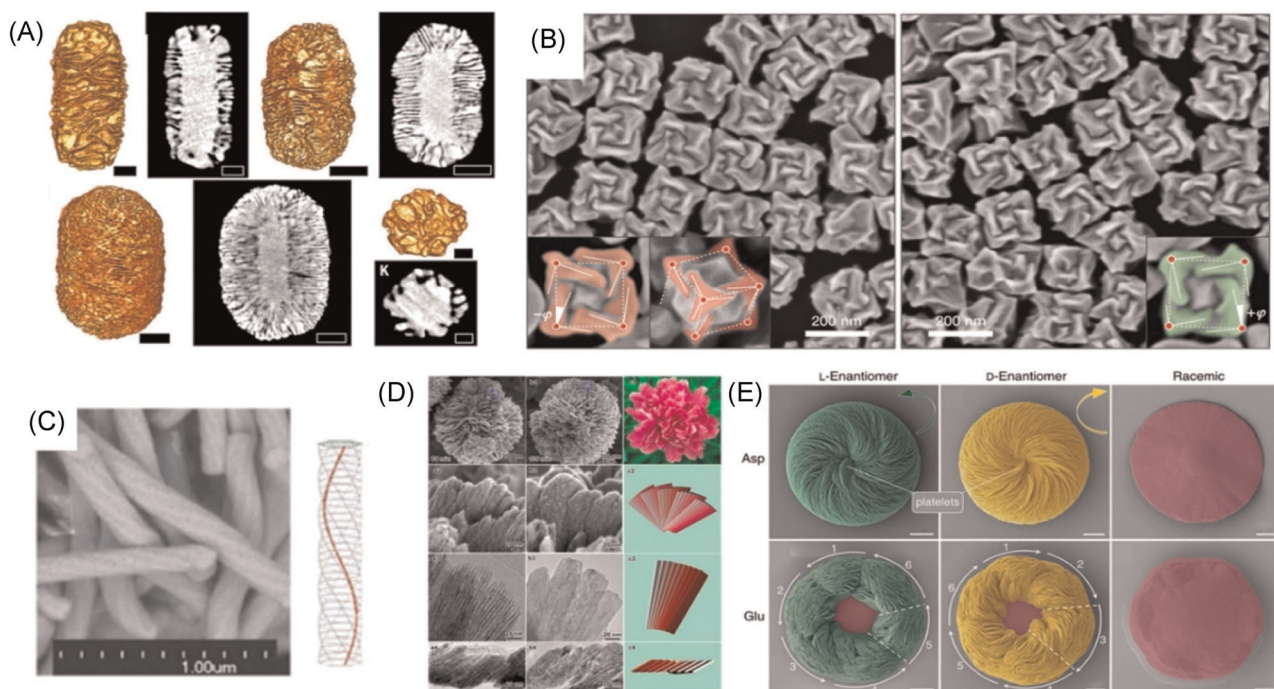


**FIGURE 5** Some representative chiral nanoparticles. (A) Au nanorod with spiral wrinkles. Adapted with permission.<sup>80</sup> Copyright 2020, AAAS. (B) Au helicoid. Adapted with permission.<sup>81</sup> Copyright 2018, Springer Nature. (C) Silica. Adapted with permission.<sup>83</sup> Copyright 2004, Springer Nature. (D) CuO. Adapted with permission.<sup>84</sup> Copyright 2014, ACS. (E)  $\text{CaCO}_3$ . Adapted with permission.<sup>85</sup> Copyright 2017, Springer Nature

The obtained Au NPs featured very high dissymmetry factors ( $\sim 0.20$ ), which was higher than in some organics. The organic ligands influenced the diffusion and deposition manner of newly formed Au atoms, which resulted in the growth of spiral wrinkles around the seeds. Amino acids could also be employed to direct the formation of chiral Au NPs. Lee et al.<sup>81,82</sup> reported the fabrication of twisted Au nanocubes (helicoid, Figure 5B) or octahedra with strong chiral plasmonic optical activity. The structural evolution process could mimic the biogenesis of chiral objects, in which the structure varied along time and spiral structures gradually expanded.<sup>9</sup>

Such “indirect transfer” process has also been observed in other material systems,<sup>86,87</sup> such as zeolites and MOFs,<sup>88</sup> silica,<sup>83</sup> CuO,<sup>84</sup> ZnO,<sup>89</sup> TiO<sub>2</sub>,<sup>90,91</sup> CaCO<sub>3</sub>,<sup>85</sup> and so forth. The common feature of these materials is that almost all of them contain spiral structures. However, the origin of these spiral structures is not all the same. Che et al.<sup>83</sup> reported the fabrication of mesoporous silica with a twisted hexagonal rod-like morphology (Figure 5C), and the growth mechanism was ascribed to the spiral surfactant-templated growth. Spiral TiO<sub>2</sub> fibers could be obtained by the transcription of helically structured amino acid-derived amphiphile fibers.<sup>90</sup> Another type of spiral structure is a hierarchical superstructure containing helically arranged nanobelts or platelets. The building blocks gradually twist with the help of amino acids, making the superstructure chiral (Figure 5D,E). In the case of cinnabar  $\alpha$ -HgS with a space group of P3<sub>2</sub>21, in which Hg and S atoms are arranged in a helical form along the crystallographic *c* axis, enantiomeric control could be realized by employing D- or L-penicillamine in the synthesis, which led to enantiopure twisted octahedrons.<sup>92</sup> But even nonchiral organic compounds can induce chirality in self-assembled inorganic structures. This was demonstrated by Yu et al.<sup>93</sup> for BaCO<sub>3</sub> nanoparticles, which self-assembled into helical superstructures via geometrical control of a stiff achiral and face selectively adsorbing block copolymer.

### 3.2 | Chirality transfer from inorganics to organics

This process mainly contains the enantioselective adsorption of organics on inorganics and the asymmetric catalysis on inorganics. The latter process usually relies on the first process. The enantioselective adsorption is decided by the stereochemistry of adsorbate and substrate. Such interaction is analogous to a 10-pin bowler's selection of left- versus right-handed ball. There are three noncollinear holes for the thumb and first two fingers in the 10-pin bowling balls, and a right-handed bowler

cannot use a left-handed ball and vice versa. This feature means that (1) the chirality of both the adsorbate and substrate should match; (2) the chemical groups in the adsorbate have strong interaction with the substrate.

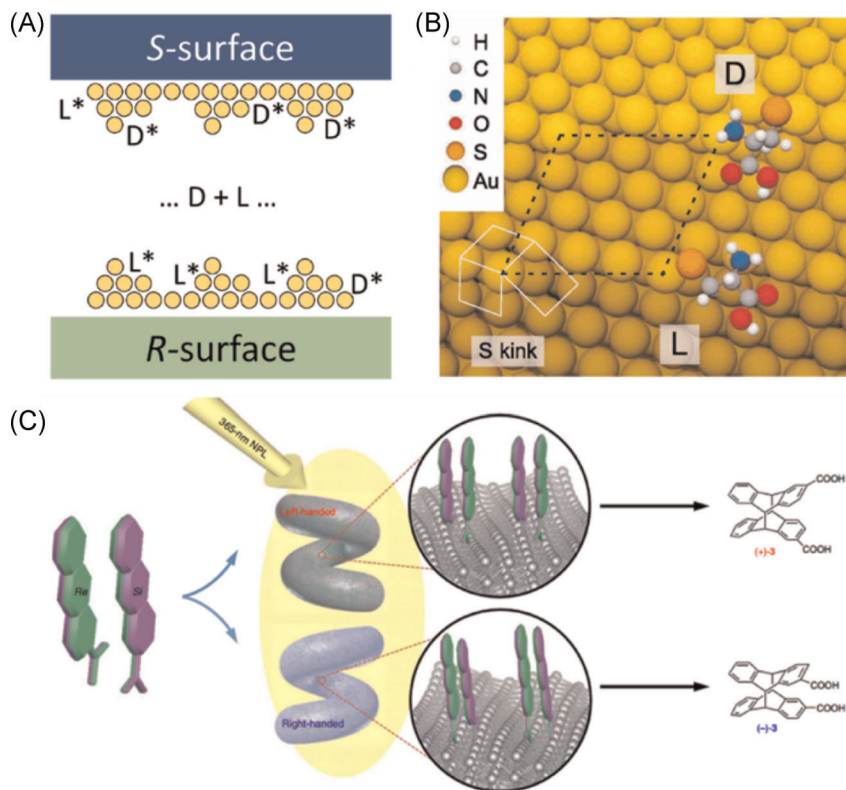
Chiral porous materials have been widely investigated in both enantioselective adsorption (for chiral resolution), as well as asymmetric catalysis. And there is a large family of different materials with different features. Readers can find useful information in these comprehensive reviews.<sup>18,94,95</sup> In this section, we would like to discuss the enantioselective adsorption and catalysis on chiral surfaces (Figure 6A).

The enantioselective adsorption on natural inorganics was confirmed a long time ago. Bonner et al.<sup>98</sup> reported the asymmetric adsorption of D- or L-alanine on quartz with different chirality in 1974, finding that the extent of the asymmetric adsorption was about 1.0%–1.4%. It is interesting to find that many natural amino acids have been found to asymmetrically adsorb on chiral minerals, which might hold a potential answer to the homochirality on Earth. For example,  $\epsilon$ -Zn(OH)<sub>2</sub> (Wulfingite) chiral crystals showed enantioselective adsorption of Arginine.<sup>99</sup> The surfaces of metals are easier to deal with as compared to minerals. Thus, chiral metal surfaces have been more explored. For the asymmetric adsorption, the desorption energies for R- and S-enantiomers on the surface should be different ( $|\Delta\Delta E_{\text{des}}|$ ). Most of the observed  $|\Delta\Delta E_{\text{des}}|$  on chiral metal surfaces ranged from  $\sim 0.0$  to 0.6 kcal/mol, and roughly a quarter of them were less than 0.1 kcal/mol. The D-cysteine would bind  $\sim 0.3$  kcal/mol stronger than L-cysteine on an S-type Au(17,11,9) surface (Figure 6B),<sup>100</sup> and such asymmetric adsorption has been confirmed by X-ray photoelectron spectroscopy.<sup>96</sup> Gellman et al.<sup>101</sup> used temperature-programmed desorption (TPD) to measure the R-3-methylcyclohexanone desorption on different chiral Cu surfaces, such as (643), (653), (651), (13,9,1), (17,5,1), (821), and (531). The  $|\Delta\Delta E_{\text{des}}|$  was found to range from  $\sim 0.63$  to 1.08 kcal/mol.<sup>101</sup> They also found that the adsorption equilibrium constants of D- or L-aspartic acid on Cu(3,1,17)<sup>R&S</sup> surfaces were around  $2.29 \pm 0.17$ , which suggested that the S-surface (or R-surface) would adsorb D-aspartic acid (or L-aspartic acid) 2.29 times stronger than L-aspartic acid (or D-aspartic acid), respectively.<sup>102</sup> However, similar experiments have been conducted with D,L-serine and D,L-phenylalanine, no asymmetric adsorption has been found on Cu(3,1,17)<sup>R&S</sup> surfaces. The results suggested that such enantioselectivity required functional groups strongly interacting with the surface.<sup>103</sup>

Adsorption is usually the first step toward catalytic reactions. Once the adsorbate has been selectively adsorbed on the surface, asymmetric catalysis could be foreseen. It has been demonstrated that chiral quartz promotes the chiral synthesis of pyrimidyl alkanol with a chiral excess of 93%–97%.<sup>104</sup> In another case, the different adsorption could



**FIGURE 6** (A) Schematic illustration of the enantioselective adsorption of D- or L- type enantiomers on different chiral surfaces. (B) Atomic model of D- or L- cysteine adsorption on an S-type Au(17,11,9) surface. Adapted with permission.<sup>96</sup> Copyright 2007, APS. (C) Structural matching of intermediates on chiral surfaces. Adapted with permission.<sup>97</sup> Copyright 2020, Springer Nature



contribute to a 0.33-kcal/mol difference in activation energy in the electrooxidation of D- and L-glucose on Pt(643)<sup>S</sup> surfaces, which resulted in a molar percentage of the major diastereomeric product of 64%.<sup>105</sup> The enantioselective catalysis was more obvious in the R,R- and S,S-tartaric acid decomposition on a chiral Cu surface, with reaction rates that differed by as much as two orders of magnitude, even though the effective rate constants for decomposition differed by less than a factor of 2.<sup>106</sup>

The selective adsorption of not only reactants but also intermediates can lead to asymmetric catalysis. In a recent study, Wei et al. found that a prochiral molecule, 2-anthracenecarboxylic acid, could stereoselectively adsorb on the metal nanohelices in the form of enantiomorphous anti-head-to-head dimers (Figure 6C), which resulted in a specific enantiopreference during their photoinduced cyclodimerization.<sup>97</sup> The enantiomeric excess ranged from  $-5.5\%$  to  $4.0\%$ , according to the structures of the nanohelices.

## 4 | OUTLOOK AND PERSPECTIVES

Many aspects of chiral communications can be specially emphasized from the perspective of inorganic materials (Figure 7). At this stage, investigating the chirality communication between organics and inorganics mainly aims to establish methods to prepare chiral inorganics

with high quality, as well as asymmetric catalysis. Developing robust, reproducible, and low-cost methods and methodology to the high-quality synthesis is always the first step, and maybe the most important step, toward both fundamental investigations and applications. Moreover, efficient separation methods are also helpful in improving the quality of the materials. And at last, we

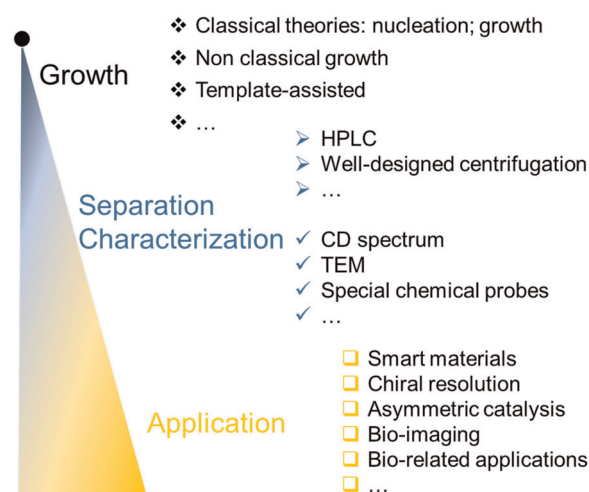


**FIGURE 7** Aspects that could be emphasized from the perspective of inorganic materials. CD, circular dichroism; HPLC, high-performance liquid chromatography; TEM, transmission electron microscopy

can make good use of the materials. Here, we would give some personal perspectives on several aspects of the communications.

#### 4.1 | Growth methods

There are many different strategies to prepare chiral inorganics now,<sup>3,107</sup> such as template growth, glancing angle deposition, chiral biomineralization, and chiral imprinting, and so forth. Different strategies can be used in different material systems. As it has been mentioned previously, only a small part of organics can crystallize in an enantiopure way, and the heterogeneous interaction across the molecules is the key to the crystallization.<sup>36</sup> Here, we would like to provide more views on the wet-chemical synthesis from the perspective of the classical nucleation theory. The points discussed here might help to enlarge the library of chiral inorganic NPs.

For materials with chiral organics in their lattice, the enantiopure products could be readily obtained with enantiopure organics as precursors. The following crystal phase control, composition control, and morphology control follow the conventional crystal growth strategies.

For materials with intrinsic chiral lattices, thermodynamic control during the growth process might help to obtain enantiopure products. Chiral capping agents, which can bind with certain geometry on the materials, might help to produce chiral inorganics. Now the most used capping agents are mainly amino acids and peptides, maybe because they are quite accessible. The interactions between inorganics and amino acids or peptides are actually very complicated due to the multiple functional groups and versatile conformation of the organics. The  $-NH_2$  and  $-COOH$  can help all bind with the surface. Thus, they can serve as monodentate or bidentate ligands in the process, and the binding interaction can be largely influenced by pH values as well. When cysteine is used in the process, the  $-SH$  group might also bind with the inorganics, which adds extra difficulties in understanding the process. Moreover, disulfide bonds can also form in the synthesis. To simplify the process, some simpler chiral ligands are suggested to be used, such as 2-butanol, 2-aminobutane, 1,2-propanediol, 2-amino-1-butanol, 3-amino-1,2-propanediol, 1,1'-bi(2-naphthol), 1,1'-binaphthyl-2,2'-diamine, and so forth, which are also accessible from chemical agent companies.

For materials without chiral lattices, controlling the growth kinetics is potentially more useful than thermodynamics. The nuclei (3D or 2D nuclei) of the crystals must be chiral if the final structures are chiral. Thus, making the nuclei chiral should be a possible method to obtain chiral NPs. In classical nucleation and growth

theory, the nucleation rate ( $J_0$ ) can be roughly expressed by:

$$J_0 = K \exp\left(\frac{-\Delta G^*}{kT}\right), \quad (1)$$

where  $K$  is the pre-exponential,  $k$  is the Boltzmann constant,  $T$  is the temperature, and  $\Delta G^*$  is the energy barrier of the critical nuclei.

The nucleation rate is relatively slow according to this equation, which makes the control over nuclei possible. If chiral additives are present, nucleation of one enantiomer can be favored over that of the other simply because the additives can act as chiral promotor or inhibitor, which would influence the nucleation of the two enantiomers in a different way as well as  $\Delta G^*$ . The structures of the nuclei are dynamic and can ripen and change their shape easily.<sup>108–110</sup> If some chiral ligands interact strongly with the nuclei, it would additionally be possible that the following growth would amplify such asymmetry, and eventually, chiral NPs would be obtained.

However, there are chemical reactions before nucleation in many syntheses, such as Au(0) atom formation before Au NP formation. In this case, the nucleation rate could be expressed as follows:

$$J_0 = K \exp\left(\frac{-\Delta E}{kT}\right) \exp\left(\frac{-\Delta G^*}{kT}\right) = K \exp\left(\frac{-\Delta E - \Delta G^*}{kT}\right), \quad (2)$$

where  $\Delta E$  is the energy change of the building block formation process before the nucleation. Accordingly, the energy barrier of nucleation would be easily overcome in the synthesis, and the nucleation would be really fast, which makes controlling the nuclei difficult. Thus, finding a proper reaction system is vital for this strategy.

Other pathways besides the classical nucleation of chiral nanoparticles are nonclassical nucleation pathways like the prenucleation cluster pathway,<sup>111–114</sup> which was discovered for  $CaCO_3$ .<sup>115</sup> It could be shown by analytical ultracentrifugation and electrospray mass spectroscopy that all amino acids form prenucleation clusters.<sup>116</sup> Although this was revealed for racemic mixtures, tests with enantiopure arginine show that chirality does not affect the oligomer distribution, so that prenucleation clusters can be assumed for all chiral amino acids as well.<sup>116</sup> Isotope labeling of serine revealed a strong preference for homochiral aggregates,<sup>117–121</sup> showing that amino acids can distinguish between their enantiomers upon oligomer formation.<sup>122,123</sup> Therefore, chiral nuclei can be formed by the prenucleation cluster pathway.

Another nonclassical nucleation pathway is the two-step nucleation found for proteins.<sup>124,125</sup> Here, a dense

liquid phase is formed first as a precursor to the crystal. As proteins are built up from L-amino acids, they are chiral and form chiral crystals. These two examples show that nonclassical nucleation pathways are promising alternatives to classical nucleation of chiral crystals.

A special case of crystal growth is the screw dislocation-driven growth. The screw dislocation can provide nonvanishing steps on the crystal surface, which bypasses the further nucleation on the surface during growth. Such screw dislocation growth method usually leads to spiral or helical morphologies.<sup>126,127</sup> When the chirality of the screw dislocation is controlled, enantiopure inorganic nanomaterials could be obtained.<sup>128,129</sup>

Another point we can get from controlling nucleation is that the number of chiral ligands required in the synthesis should be small as the size of the nuclei is small, and the atomic ratio of the nuclei to all the metal atoms is small. To some extent, this also explains why a trace amount of impurities could dramatically influence some synthesis processes.<sup>130</sup>

## 4.2 | Separations and characterizations

Separation or chiral resolution of inorganic NPs is quite difficult as the chiral high-performance liquid chromatography methods using imprinted columns for organic molecules would not work for chiral NPs due to their much larger size. The best way to obtain enantiopure NPs is by controlling the growth. Suppose the chirality of single NPs has been well controlled in the synthesis, then the separation just aims to separate different shapes. In that case, proper centrifugation might be enough for the purpose. Centrifugation in solutions containing proper chiral ligands might also help to purify the NPs further as the interaction between ligands and different NPs might differ as their geometry fitness differs. It has been found that preparative density gradient ultracentrifugation could be applied to separate racemate crystals from excess enantiomer crystals. This was demonstrated for alanine crystals separated in a 50 wt% Nycodenz gradient. The recovery rates of the pure enantiomers from the mixtures were good (70%–90%).<sup>38</sup> This method provides a promising tool for purifying chiral NPs.

However, (ultra)centrifugation could potentially play a much bigger role for the analysis of chiral NPs, but also for their separation. The key would be to establish and quantify the chiral interaction of chiral solvents or non-sedimenting chiral solutes with chiral NPs. If this interaction can be tuned and made sufficiently strong by the variation of experimental parameters like temperature, concentration, pH, and so forth. Then it can be expected

that the sedimentation velocity of the two enantiomers in a racemic NP mixture would be sufficiently different to allow for an effective and upscalable separation via differential sedimentation. But even rate-zonal centrifugation experiments could be adapted accordingly using a dissolved chiral component like a chiral sugar in differently concentrated layers. Besides, the preparative separation, analytical ultracentrifugation of chiral NPs would allow for the quantification of their chiral interactions with either the solvent or dissolved chiral compounds. This could reveal the equilibrium constant and with it the free enthalpy as well as the stoichiometry of the interaction and thus establish a very valuable analytical tool for the analysis of chiral interactions as, in the analytical ultracentrifuge, all NPs are detected so that the obtained results are statistically relevant. This could be the key to investigate the chiral communication not only between inorganic NPs and chiral molecules.

Now chiroptical properties are mainly used as the index to confirm the chirality, which is characterized by circular dichroism (CD) spectrum. This index is very suitable for optical applications. However, the spectrum is not efficient in chiral structures with weak optical activity. Transition electron microscopy or other morphology characterization methods can be applied to visualize the chiral shape. But they can only give information on a limited number of NPs, and the atomic structures are hard to describe sometimes. Thus, more kinds of characterization methods are highly appreciated. For example, chiral surfaces, which are active in asymmetric catalysis, might show weak peaks in the CD spectrum, and their atomic structures are difficult to capture. To find better asymmetric catalysts or establish new methodologies for asymmetric catalysis, some new chiral chemical probes need to be developed. The probes should contain similar binding groups with the reactants and could report the efficiency of the binding with catalysts in some way (such as UV-Vis spectrum, CD spectrum, or fluorescence spectrum). It would be nice if the binding group is a common functional group in organics and can be catalyzed to other useful intermediates or products. Such probes would greatly contribute to the exploration of asymmetric catalysis.

## 4.3 | Applications

Different materials are suitable for different applications. Materials with intrinsically chiral lattice might be suitable for studying their physical properties, which can contribute to both fundamental science and new smart material design. The asymmetric geometry, like twisted or helical structures, might help to amplify the

performance of these kinds of materials. This is a multidisciplinary research field and requires collaboration and contributions from different research fields.

Asymmetric catalysis by using chiral inorganic materials is a relatively new field with a fascinating future. The current researched materials are mainly achiral inorganics@chiral environments, such as Fe<sub>3</sub>O<sub>4</sub> NPs modified by chiral Ru complexes, which showed promising activities in heterogeneous asymmetric hydrogenation of aromatic ketones,<sup>131</sup> 2,2'-bis(diphenylphosphino)-1,1'-binaphthene modified FePd NPS, which could catalyze asymmetric coupling reactions,<sup>132</sup> and so forth. As for asymmetric photocatalysis, there are two effective strategies. The first one combines both heterogeneous semiconductor catalysts and homogenous chiral catalysts, whereas the second one integrates both photoactive component and chiral catalyst in a bifunctional system.<sup>133</sup> Many novel systems have been designed based on these two strategies, such as TiO<sub>2</sub>-ligand systems,<sup>134,135</sup> quantum dot-chiral ligand systems,<sup>136,137</sup> and so forth. Meanwhile, MOF and COF materials have been found promising in these reactions due to their versatile functional groups. For example, chiral metallosalen<sup>138,139</sup> and 1,1'-bi-2-naphthol-type chiral ligand<sup>140</sup> have been employed in chiral MOF catalysts.

The explored systems mainly utilize the chiral environments to induce enantioselective reactions. On the contrary, chiral surfaces should be able to serve as a chiral catalyst as well.<sup>97</sup> This field deserves more research. Besides normal thermocatalysis reactions, electrocatalysis is now emerging as another powerful method. The polarization effect of an applied potential can exert an influence on the electron donor or withdraw center, essentially acting as a tunable functional group. This property offers new dimensions for selective catalysis.<sup>141</sup> Moreover, the chiral electrodes can also tune the spin of charges, which might be useful in asymmetric catalysis.<sup>142</sup> Comparing the stereochemistry of chiral surfaces with organics or biomolecules, they should be promising in bioapplications as well.<sup>143</sup> For example, chiral Au NPs have been used in detecting myloids in Parkinson's and prion diseases,<sup>144</sup> or inhibiting A $\beta$  fibrillation, which is highly related to Alzheimer's disease.<sup>145</sup> When the inorganic chiral toolbox has been enriched and their communication with organics has been well studied, more novel and useful applications can be expected.

## 5 | CONCLUSION

In summary, there are many challenges, as well as opportunities, in the chirality communication between inorganics and organics. The challenges mainly arise from the limited

number of chiral inorganics and the lack of efficient methods to control the morphology of inorganics, which necessitate a better understanding of the chirality transfer from organics to inorganics. At the current stage, chirality transfer and recognition are the main drivers of chiral communications, and they sometimes coexist in the process. It is foreseeable that more communication manners, bridged by novel physical properties of organics and inorganics, can be developed when the library of chiral inorganics has been enlarged, such as in spintronics, quantum networks, and computing, and so forth.

## ACKNOWLEDGMENTS

Bing Ni thank the Alexander von Humboldt Foundation for financial support.

## CONFLICT OF INTERESTS

The authors declare that there are no conflict of interests.

## ORCID

Bing Ni  <https://orcid.org/0000-0001-9657-6933>

Helmut Cölfen  <https://orcid.org/0000-0002-1148-0308>

## REFERENCES

1. Visheratina A, Kotov NA. Inorganic Nanostructures with strong chiroptical activity. *CCS Chem.* 2020;2:583-604.
2. Kuang H, Xu C, Tang Z. Emerging chiral materials. *Adv Mater.* 2020;32:2005110.
3. Shukla N, Gellman AJ. Chiral metal surfaces for enantioselective processes. *Nat Mater.* 2020;19:939-945.
4. Ma W, Xu L, de Moura AF, et al. Chiral inorganic nanostructures. *Chem Rev.* 2017;117:8041-8093.
5. Im SW, Ahn HY, Kim RM, et al. Chiral surface and geometry of metal nanocrystals. *Adv Mater.* 2020;32:1905758.
6. Gal J. Pasteur and the art of chirality. *Nat Chem.* 2017;9:604-605.
7. Molčanov K, Stilinović V. Chemical crystallography before X-ray diffraction. *Angew Chem Int Ed.* 2014;53:638-652.
8. Kahr B, Arteaga O. Arago's best paper. *ChemPhysChem.* 2012;13:79-88.
9. Ahn H-Y, Yoo S, Cho NH, et al. Bioinspired toolkit based on intermolecular encoder toward evolutionary 4D chiral plasmonic materials. *Acc Chem Res.* 2019;52:2768-2783.
10. Kennedy D, Norman C. What don't we know. *Science.* 2005;309:75.
11. Hazen RM, Sholl DS. Chiral selection on inorganic crystalline surfaces. *Nat Mater.* 2003;2:367-374.
12. Hendricks MP, Sato K, Palmer LC, Stupp SI. Supramolecular assembly of peptide amphiphiles. *Acc Chem Res.* 2017;50:2440-2448.
13. Aggeli A, Nyrkova IA, Bell M, et al. Hierarchical self-assembly of chiral rod-like molecules as a model for peptide  $\beta$ -sheet tapes, ribbons, fibrils, and fibers. *Proc Natl Acad Sci.* 2001;98:11857-11862.
14. Luo Z, Zhang S. Designer nanomaterials using chiral self-assembling peptide systems and their emerging benefit for society. *Chem Soc Rev.* 2012;41:4736-4754.

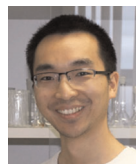
15. Tahara K, Yamaga H, Ghijsens E, et al. Control and induction of surface-confined homochiral porous molecular networks. *Nat Chem*. 2011;3:714-719.
16. Destoop I, Ghijsens E, Katayama K, et al. Solvent-induced homochirality in surface-confined low-density nanoporous molecular networks. *J Am Chem Soc*. 2012;134:19568-19571.
17. Chen T, Yang W-H, Wang D, Wan L-J. Globally homochiral assembly of two-dimensional molecular networks triggered by co-absorbers. *Nat Commun*. 2013;4:1389.
18. Sun Z, Hou J, Li L, Tang Z. Nanoporous materials for chiral resolution. *Coord Chem Rev*. 2020;425:213481.
19. Fan Y, Zhang J, Shen Y, et al. Emerging porous nanosheets: from fundamental synthesis to promising applications. *Nano Res*. 2020;14:1-28. <https://doi.org/10.1007/s12274-12020-13082-12274>
20. Jiao L, Wang Y, Jiang HL, Xu Q. Metal-organic frameworks as platforms for catalytic applications. *Adv Mater*. 2018;30:1703663.
21. Jiao L, Seow JYR, Skinner WS, Wang ZU, Jiang H-L. Metal-organic frameworks: structures and functional applications. *Mater Today*. 2019;27:43-68.
22. Long G, Sabatini R, Saidaminov MI, et al. Chiral-perovskite optoelectronics. *Nat Rev Mater*. 2020;5:423-439.
23. Sholl DS, Asthagiri A, Power TD. Naturally chiral metal surfaces as enantiospecific adsorbents. *J Phys Chem B*. 2001;105:4771-4782.
24. Zhang S, Shi W, Rong S, Li S, Zhuang J, Wang X. Chirality evolution from sub-1 nanometer nanowires to the macroscopic helical structure. *J Am Chem Soc*. 2020;142:1375-1381.
25. Nakagawa M, Kawai T. Chirality-controlled syntheses of double-helical Au nanowires. *J Am Chem Soc*. 2018;140:4991-4994.
26. Ben-Moshe A, Maoz BM, Govorov AO, Markovich G. Chirality and chiroptical effects in inorganic nanocrystal systems with plasmon and exciton resonances. *Chem Soc Rev*. 2013;42:7028-7041.
27. Okano K, Arteaga O, Ribo JM, Yamashita T. Emergence of chiral environments by effect of flows: the case of an ionic oligomer and Congo red dye. *Chem Eur J*. 2011;17:9288-9292.
28. Okano K, Yamashita T. Formation of chiral environments by a mechanical induced vortex flow. *ChemPhysChem*. 2012;13:2263-2271.
29. Sun J, Li Y, Yan F, et al. Control over the emerging chirality in supramolecular gels and solutions by chiral microvortices in milliseconds. *Nat Commun*. 2018;9:2599.
30. Tan C, Qi X, Liu Z, et al. Self-assembled chiral nanofibers from ultrathin low-dimensional nanomaterials. *J Am Chem Soc*. 2015;137:1565-1571.
31. Kim J-Y, Yeom J, Zhao G, et al. Assembly of gold nanoparticles into chiral superstructures driven by circularly polarized light. *J Am Chem Soc*. 2019;141:11739-11744.
32. Yeom J, Yeom B, Chan H, et al. Chiral templating of self-assembling nanostructures by circularly polarized light. *Nat Mater*. 2015;14:66-72.
33. Robbie K, Brett M, Lakhtakia A. Chiral sculptured thin films. *Nature*. 1996;384:616-616.
34. Singh G, Chan H, Baskin A, et al. Self-assembly of magnetite nanocubes into helical superstructures. *Science*. 2014;345:1149-1153.
35. Kondepudi DK, Crook KE. Theory of conglomerate crystallization in the presence of chiral impurities. *Cryst Growth Des*. 2005;5:2173-2179.
36. Carpenter JE, Grünwald M. Heterogeneous interactions promote crystallization and spontaneous resolution of chiral molecules. *J Am Chem Soc*. 2020;142:10755-10768.
37. Mastai Y, Sedláč M, Cölfen H, Antonietti M. The separation of racemic crystals into enantiomers by chiral block copolymers. *Chem Eur J*. 2002;8:2429-2437.
38. Mastai Y, Völkel A, Cölfen H. Separation of racemate from excess enantiomer of chiral nonracemic compounds via density gradient ultracentrifugation. *J Am Chem Soc*. 2008;130:2426-2427.
39. Feringa BL, van Delden RA, Koumura N, Geertsema EM. Chiroptical molecular switches. *Chem Rev*. 2000;100:1789-1816.
40. Tong S, Li J-T, Liang D-D, et al. Catalytic enantioselective synthesis and switchable chiroptical property of inherently chiral macrocycles. *J Am Chem Soc*. 2020;142:14432-14436.
41. Katsonis N, Lancia F, Leigh DA, Pirvu L, Ryabchun A, Schaufelberger F. Knotting a molecular strand can invert macroscopic effects of chirality. *Nat Chem*. 2020;12:939-944.
42. Ceconello A, Lu C-H, Elbaz J, Willner I. Au nanoparticle/DNA rotaxane hybrid nanostructures exhibiting switchable fluorescence properties. *Nano Lett*. 2013;13:6275-6280.
43. Li N, Tittl A, Yue S, et al. DNA-assembled bimetallic plasmonic nanosensors. *Light: Sci Appl*. 2014;3:e226.
44. Klös G, Andersen A, Miola M, Birkedal H, Sutherland DS. Oxidation controlled lift-off of 3D chiral plasmonic Au nanohooks. *Nano Res*. 2019;12:1635-1642.
45. Morisawa K, Ishida T, Tatsuma T. Photoinduced chirality switching of metal-inorganic plasmonic nanostructures. *ACS Nano*. 2020;14:3603-3609.
46. Zhuang T-T, Li Y, Gao X, et al. Regioselective magnetization in semiconducting nanorods. *Nat Nanotechnol*. 2020;15:192-197.
47. Baimuratov AS, Rukhlenko ID, Noskov RE, et al. Giant optical activity of quantum dots, rods, and disks with screw dislocations. *Sci Rep*. 2015;5:14712.
48. Billing DG, Lemmerer A. Bis [(S)- $\beta$ -phenethylammonium] tribromoplumbate (II). *Acta Crystallogr Sect E: Struct Rep Online*. 2003;59:m381-m383.
49. Ahn J, Lee E, Tan J, Yang W, Kim B, Moon J. A new class of chiral semiconductors: chiral-organic-molecule-incorporating organic-inorganic hybrid perovskites. *Mater Horiz*. 2017;4:851-856.
50. Ahn J, Ma S, Kim J-Y, et al. Chiral 2D organic-inorganic hybrid perovskite with circular dichroism tunable over wide wavelength range. *J Am Chem Soc*. 2020;142:4206-4212.
51. Ma J, Fang C, Chen C, et al. Chiral 2D perovskites with a high degree of circularly polarized photoluminescence. *ACS Nano*. 2019;13:3659-3665.
52. Chen C, Gao L, Gao W, et al. Circularly polarized light detection using chiral hybrid perovskite. *Nat Commun*. 2019;10:1927.
53. Long G, Jiang C, Sabatini R, et al. Spin control in reduced-dimensional chiral perovskites. *Nat Photonics*. 2018;12:528-533.
54. Lu H, Xiao C, Song R, et al. Highly distorted chiral two-dimensional tin iodide perovskites for spin-polarized charge transport. *J Am Chem Soc*. 2020;142:13030-13040.
55. Yang CK, Chen WN, Ding YT, et al. The first 2D homochiral lead iodide perovskite ferroelectrics: [R- and S-1-(4-chlorophenyl) ethylammonium]  $_2$ PbI $_4$ . *Adv Mater*. 2019;31:1808088.

56. Deng B-B, Xu C-C, Cheng T-T, et al. Homochiral nickel nitrite  $ABX_3$  ( $X=NO_2^-$ ) perovskite ferroelectrics. *J Am Chem Soc.* 2020;142:6946-6950.
57. Yuan C, Li X, Semin S, Feng Y, Rasing T, Xu J. Chiral lead halide perovskite nanowires for second-order nonlinear optics. *Nano Lett.* 2018;18:5411-5417.
58. Seo JS, Whang D, Lee H, et al. A homochiral metal-organic porous material for enantioselective separation and catalysis. *Nature.* 2000;404:982-986.
59. Chen X, Qiao Z, Hou B, et al. Chiral metal-organic frameworks with tunable catalytic selectivity in asymmetric transfer hydrogenation reactions. *Nano Res.* 2020;14:466-472. <https://doi.org/10.1007/s12274-12020-12905-12277>
60. Moloney MP, Gun'ko YK, Kelly JM. Chiral highly luminescent CdS quantum dots. *Chem Commun.* 2007;:3900-3902.
61. Xiao L, An T, Wang L, Xu X, Sun H. Novel properties and applications of chiral inorganic nanostructures. *Nano Today.* 2020;30:100824.
62. Gao X, Han B, Yang X, Tang Z. Perspective of chiral colloidal semiconductor nanocrystals: opportunity and challenge. *J Am Chem Soc.* 2019;141:13700-13707.
63. Zhou Y, Zhu Z, Huang W, et al. Optical coupling between chiral biomolecules and semiconductor nanoparticles: size-dependent circular dichroism absorption. *Angew Chem Int Ed.* 2011;123:11658-11661.
64. Tohgha U, Deol KK, Porter AG, et al. Ligand-induced circular dichroism and circularly polarized luminescence in CdSe quantum dots. *ACS Nano.* 2013;7:11094-11102.
65. Zhou Y, Yang M, Sun K, Tang Z, Kotov NA. Similar topological origin of chiral centers in organic and nanoscale inorganic structures: effect of stabilizer chirality on optical isomerism and growth of CdTe nanocrystals. *J Am Chem Soc.* 2010;132:6006-6013.
66. Nordén B, Rodger A, Dafforn T. *Linear dichroism and circular dichroism: a textbook on polarized-light spectroscopy.* London, UK: Royal Society of Chemistry; 2010.
67. Zhang H, He H, Jiang X, Xia Z, Wei W. Preparation and characterization of chiral transition-metal dichalcogenide quantum dots and their enantioselective catalysis. *ACS Appl Mater Inter.* 2018;10:30680-30688.
68. Schaaff TG, Knight G, Shafiqullin MN, Borkman RF, Whetten RL. Isolation and selected properties of a 10.4 kDa gold: glutathione cluster compound. *J Phys Chem B.* 1998;102:10643-10646.
69. Li Y, Higaki T, Du X, Jin R. Chirality and surface bonding correlation in atomically precise metal nanoclusters. *Adv Mater.* 2020;32:1905488.
70. Han Z, Zhao X, Peng P, et al. Intercluster aurophilicity-driven aggregation lighting circularly polarized luminescence of chiral gold clusters. *Nano Res.* 2020;13:3248-3252.
71. Zeng C, Chen Y, Kirschbaum K, Lambright KJ, Jin R. Emergence of hierarchical structural complexities in nanoparticles and their assembly. *Science.* 2016;354:1580-1584.
72. Zeng C, Liu C, Chen Y, Rosi NL, Jin R. Gold-thiolate ring as a protecting motif in the  $Au_{20}(SR)_{16}$  nanocluster and implications. *J Am Chem Soc.* 2014;136:11922-11925.
73. Qian H, Eckenhoff WT, Zhu Y, Pintauer T, Jin R. Total structure determination of thiolate-protected Au<sub>38</sub> nanoparticles. *J Am Chem Soc.* 2010;132:8280-8281.
74. Knoppe S, Bürgi T. Chirality in thiolate-protected gold clusters. *Acc Chem Res.* 2014;47:1318-1326.
75. Dolamic I, Knoppe S, Dass A, Bürgi T. First enantioseparation and circular dichroism spectra of Au<sub>38</sub> clusters protected by achiral ligands. *Nat Commun.* 2012;3:798.
76. Hasenknopf B, Micoine K, Lacôte E, Thorimbert S, Malacria M, Thouvenot R. Chirality in polyoxometalate chemistry. *Eur J Inorg Chem.* 2008;2008:5001-5013.
77. Schunack M, Lægsgaard E, Stensgaard I, Johannsen I, Besenbacher F. A chiral metal surface. *Angew Chem Int Ed.* 2001;40:2623-2626.
78. Schunack M, Petersen L, Kühnle A, et al. Anchoring of organic molecules to a metal surface: HtBDC on Cu (110). *Phys Rev Lett.* 2001;86:456-459.
79. Chen Q, Richardson NV. Surface faceting induced by adsorbates. *Prog Surf Sci.* 2003;73:59-77.
80. González-Rubio G, Mosquera J, Kumar V, et al. Micelle-directed chiral seeded growth on anisotropic gold nanocrystals. *Science.* 2020;368:1472-1477.
81. Lee H-E, Ahn H-Y, Mun J, et al. Amino-acid-and peptide-directed synthesis of chiral plasmonic gold nanoparticles. *Nature.* 2018;556:360-365.
82. Lee H-E, Kim RM, Ahn H-Y, et al. Cysteine-encoded chirality evolution in plasmonic rhombic dodecahedral gold nanoparticles. *Nat Commun.* 2020;11:263.
83. Che S, Liu Z, Ohsuna T, Sakamoto K, Terasaki O, Tatsumi T. Synthesis and characterization of chiral mesoporous silica. *Nature.* 2004;429:281-284.
84. Duan Y, Liu X, Han L, et al. Optically active chiral CuO "nanoflowers". *J Am Chem Soc.* 2014;136:7193-7196.
85. Jiang W, Pacella MS, Athanasiadou D, et al. Chiral acidic amino acids induce chiral hierarchical structure in calcium carbonate. *Nat Commun.* 2017;8:15066.
86. Li Y, Wang X, Miao J, et al. Chiral transition metal oxides: synthesis, chiral origins, and perspectives. *Adv Mater.* 2020;32:1905585.
87. Hananel U, Ben-Moshe A, Tal D, Markovich G. Enantiomeric control of intrinsically chiral nanocrystals. *Adv Mater.* 2020;32:1905594.
88. Morris RE, Bu X. Induction of chiral porous solids containing only achiral building blocks. *Nat Chem.* 2010;2:353-361.
89. Duan Y, Han L, Zhang J, et al. Optically active nanostructured ZnO films. *Angew Chem Int Ed.* 2015;54:15170-15175.
90. Liu S, Han L, Duan Y, et al. Synthesis of chiral TiO<sub>2</sub> nanofibre with electron transition-based optical activity. *Nat Commun.* 2012;3:1215.
91. Zhang F, Ai J, Ding K, Duan Y, Han L, Che S. Synthesis of chiral mesostructured titanium dioxide films. *Chem Commun.* 2020;56:4848-4851.
92. Wang P-p YuS-J, Govorov AO, Ouyang M. Cooperative expression of atomic chirality in inorganic nanostructures. *Nat Commun.* 2017;8:14312.
93. Yu S-H, Cölfen H, Tauer K, Antonietti M. Tectonic arrangement of BaCO<sub>3</sub> nanocrystals into helices induced by a racemic block copolymer. *Nat Mater.* 2005;4:51-55.
94. Qiu X, Zhang Y, Zhu Y, et al. Applications of nanomaterials in asymmetric photocatalysis: recent progress, challenges, and opportunities. *Adv Mater.* 2020;2001731.

95. Wang C, Zheng M, Lin W. Asymmetric catalysis with chiral porous metal-organic frameworks: critical issues. *J Phys Chem Lett.* 2011;2:1701-1709.
96. Schillinger R, Šljivančanin Ž, Hammer B, Greber T. Probing enantioselectivity with X-ray photoelectron spectroscopy and density functional theory. *Phys Rev Lett.* 2007;98:136102.
97. Wei X, Liu J, Xia G-J, et al. Enantioselective photoinduced cyclodimerization of a prochiral anthracene derivative adsorbed on helical metal nanostructures. *Nat Chem.* 2020;12:551-559.
98. Bonner WA, Kavasmaneck PR, Martin FS, Flores JJ. Asymmetric adsorption of alanine by quartz. *Science.* 1974;186:143-144.
99. Otis G, Nassir M, Zutta M, et al. Enantioselective crystallization of chiral inorganic crystals of  $\epsilon$ -Zn(OH)<sub>2</sub> with amino acids. *Angew Chem Int Ed.* 2020;59(47):20924-20929. <https://doi.org/10.1002/anie.202009061>
100. Greber T, Šljivančanin Ž, Schillinger R, Wider J, Hammer B. Chiral recognition of organic molecules by atomic kinks on surfaces. *Phys Rev Lett.* 2006;96:056103.
101. Gellman AJ, Huang Y, Koritnik AJ, Horvath JD. Structure-sensitive enantiospecific adsorption on naturally chiral Cu (hkl) R&S surfaces. *J Phys: Condens Matter.* 2016;29:034001.
102. Yun Y, Gellman AJ. Enantioselective separation on naturally chiral metal surfaces: D, L-aspartic acid on Cu {3, 1, 17} R&S surfaces. *Angew Chem Int Ed.* 2013;52:3394-3397.
103. Yun Y, Gellman AJ. Enantiospecific adsorption of amino acids on naturally chiral Cu {3, 1, 17} R&S surfaces. *Langmuir.* 2015;31:6055-6063.
104. Soai K, Osanai S, Kadowaki K, Yonekubo S, Shibata T, Sato I. D- and L-quartz-promoted highly enantioselective synthesis of a chiral organic compound. *J Am Chem Soc.* 1999;121:11235-11236.
105. Attard GA, Ahmadi A, Feliu J, et al. Temperature effects in the enantiomeric electro-oxidation of d- and l-glucose on Pt {643}<sup>s</sup>. *J Phys Chem B.* 1999;103:1381-1385.
106. Gellman AJ, Huang Y, Feng X, Pushkarev VV, Holsclaw B, Mhatre BS. Superenantioselective chiral surface explosions. *J Am Chem Soc.* 2013;135:19208-19214.
107. Fan J, Kotov NA, Chiral. Nanoceramics. *Adv Mater.* 2020;32:1906738.
108. Cao K, Biskupek J, Stoppiello CT, et al. Atomic mechanism of metal crystal nucleus formation in a single-walled carbon nanotube. *Nat Chem.* 2020;12:921-928.
109. Yang J, Zeng Z, Kang J, et al. Formation of two-dimensional transition metal oxide nanosheets with nanoparticles as intermediates. *Nat Mater.* 2019;18:970-976.
110. Liu J, Shi W, Ni B, et al. Incorporation of clusters within inorganic materials through their addition during nucleation steps. *Nat Chem.* 2019;11:839-845.
111. Gebauer D. How can additives control the early stages of mineralisation? *Minerals.* 2018;8:179.
112. Gebauer D, Kellermeier M, Gale JD, Bergström L, Cölfen H. Pre-nucleation clusters as solute precursors in crystallisation. *Chem Soc Rev.* 2014;43:2348-2371.
113. Gebauer D, Cölfen H. Prenucleation clusters and non-classical nucleation. *Nano Today.* 2011;6:564-584.
114. Gebauer D, Raiteri P, Gale JD, Cölfen H. On classical and non-classical views on nucleation. *Am J Sci.* 2018;318:969-988.
115. Gebauer D, Völkel A, Cölfen H. Stable prenucleation calcium carbonate clusters. *Science.* 2008;322:1819-1822.
116. Kellermeier M, Rosenberg R, Moise A, Anders U, Przybylski M, Cölfen H. Amino acids form prenucleation clusters: ESI-MS as a fast detection method in comparison to analytical ultracentrifugation. *Faraday Discuss.* 2012;159:23-45.
117. Koch KJ, Gozzo FC, Nanita SC, Takats Z, Eberlin MN, Cooks RG. Chiral transmission between amino acids: chirally selective amino acid substitution in the serine octamer as a possible step in homochirogenesis. *Angew Chem Int Ed.* 2002;41:1721-1724.
118. Koch KJ, Gozzo FC, Zhang D, Eberlin MN, Cooks RG. Serine octamer metaclusters: formation, structure elucidation and implications for homochiral polymerization. *Chem Commun.* 2001:1854-1855.
119. Cooks RG, Zhang D, Koch KJ, Gozzo FC, Eberlin MN. Chiroselective self-directed octamerization of serine: implications for homochirogenesis. *Anal Chem.* 2001;73:3646-3655.
120. Julian RR, Hodyss R, Kinnear B, Jarrold MF, Beauchamp J. Nanocrystalline aggregation of serine detected by electrospray ionization mass spectrometry: origin of the stable homochiral gas-phase serine octamer. *J Phys Chem B.* 2002;106:1219-1228.
121. Counterman AE, Clemmer DE. Magic number clusters of serine in the gas phase. *J Phys Chem B.* 2001;105:8092-8096.
122. Schalley CA, Weis P. Unusually stable magic number clusters of serine with a surprising preference for homochirality. *Int J Mass Spectrom.* 2002;221:9-19.
123. Nemes P, Schlosser G, Vekey K. Amino acid cluster formation studied by electrospray ionization mass spectrometry. *J Mass Spectrom.* 2005;40:43-49.
124. Vekilov PG. The two-step mechanism of nucleation of crystals in solution. *Nanoscale.* 2010;2:2346-2357.
125. Vekilov PG. Dense liquid precursor for the nucleation of ordered solid phases from solution. *Cryst Growth Des.* 2004;4:671-685.
126. Ni B, Wang X. Edge overgrowth of spiral bimetallic hydroxides ultrathin-nanosheets for water oxidation. *Chem Sci.* 2015;6:3572-3576.
127. Meng F, Morin SA, Forticaux A, Jin S. Screw dislocation driven growth of nanomaterials. *Acc Chem Res.* 2013;46:1616-1626.
128. Orme CA, Noy A, Wierzbicki A, et al. Formation of chiral morphologies through selective binding of amino acids to calcite surface steps. *Nature.* 2001;411:775-779.
129. Li G, Jiang L, Pang S, Peng H, Zhang Z. Molybdenum trioxide nanostructures: the evolution from helical nanosheets to crosslike nanoflowers to nanobelts. *J Phys Chem B.* 2006;110:24472-24475.
130. Liz-Marzán LM, Kagan CR, Millstone JE. Reproducibility in nanocrystal synthesis? Watch out for impurities! *ACS Nano.* 2020;14:6359-6361.
131. Hu A, Yee GT, Lin W. Magnetically recoverable chiral catalysts immobilized on magnetite nanoparticles for asymmetric hydrogenation of aromatic ketones. *J Am Chem Soc.* 2005;127:12486-12487.
132. Mori K, Kondo Y, Yamashita H. Synthesis and characterization of FePd magnetic nanoparticles modified with chiral

- BINAP ligand as a recoverable catalyst vehicle for the asymmetric coupling reaction. *Phys Chem Chem Phys*. 2009; 11:8949-8954.
133. Jiang C, Chen W, Zheng W-H, Lu H. Advances in asymmetric visible-light photocatalysis, 2015–2019. *Org Biomol Chem*. 2019;17:8673-8689.
  134. Ho X-H, Kang M-J, Kim S-J, Park ED, Jang H-Y. Green organophotocatalysis. TiO<sub>2</sub>-induced enantioselective  $\alpha$ -oxyamination of aldehydes. *Catal Sci Technol*. 2011;1:923-926.
  135. Kohtani S, Kawashima A, Masuda F, et al. Chiral  $\alpha$ -hydroxy acid-coadsorbed TiO<sub>2</sub> photocatalysts for asymmetric induction in hydrogenation of aromatic ketones. *Chem Commun*. 2018;54:12610-12613.
  136. Cherevatskaya M, Neumann M, Földner S, et al. Visible-light-promoted stereoselective alkylation by combining heterogeneous photocatalysis with organocatalysis. *Angew Chem Int Ed*. 2012;51:4062-4066.
  137. Jiang Y, Wang C, Rogers CR, Kodaimati MS, Weiss EA. Regio- and diastereoselective intermolecular [2+2] cycloadditions photocatalysed by quantum dots. *Nat Chem*. 2019;11:1034-1040.
  138. Cho S-H, Ma B, Nguyen ST, Hupp JT, Albrecht-Schmitt TE. A metal-organic framework material that functions as an enantioselective catalyst for olefin epoxidation. *Chem Commun*. 2006:2563-2565.
  139. Shultz AM, Farha OK, Adhikari D, Sarjeant AA, Hupp JT, Nguyen ST. Selective surface and near-surface modification of a noncatenated, catalytically active metal-organic framework material based on Mn(salen) struts. *Inorg Chem*. 2011; 50:3174-3176.
  140. Wu C-D, Hu A, Zhang L, Lin W. A homochiral porous metal-organic framework for highly enantioselective heterogeneous asymmetric catalysis. *J Am Chem Soc*. 2005; 127:8940-8941.
  141. Heo J, Ahn H, Won J, et al. Electro-inductive effect: electrodes as functional groups with tunable electronic properties. *Science*. 2020;370:214-219.
  142. Ghosh KB, Zhang W, Tassinari F, et al. Controlling chemical selectivity in electrocatalysis with chiral CuO-coated electrodes. *J Phys Chem C*. 2019;123:3024-3031.
  143. Zhao X, Zang S-Q, Chen X. Stereospecific interactions between chiral inorganic nanomaterials and biological systems. *Chem Soc Rev*. 2020;49:2481-2503.
  144. Kumar J, Eraña H, López-Martínez E, et al. Detection of amyloid fibrils in Parkinson's disease using plasmonic chirality. *Proc Natl Acad Sci*. 2018;115:3225-3230.
  145. Hou K, Zhao J, Wang H, et al. Chiral gold nanoparticles enantioselectively rescue memory deficits in a mouse model of Alzheimer's disease. *Nat Commun*. 2020;11:4790.

## AUTHOR BIOGRAPHIES



**BING NI** received his B.S. and Ph.D. from Tsinghua University in 2014 and 2019, respectively, under the supervision of Prof. Xun Wang. He is currently a Humboldt research fellow at University of Konstanz, hosted by Prof. Helmut Cölfen. His research interests involve growth mechanisms of nanomaterials, synthesis of chiral nanostructures and responsive materials



**HELMUT CÖLFEN** is full professor for physical chemistry at the University of Konstanz. His research interests are in the area of nucleation, classical and non-classical crystallization, biomineralization, synthesis of functional polymers, directed self-assembly of nanoparticles and fractionating methods of polymer and nanoparticle analysis. His group has made contributions to high resolution particle size analysis with Angström resolution in solution, mesocrystals, nonclassical nucleation and crystallization, CaCO<sub>3</sub> crystallization, bio-inspired mineralization, synthesis of double hydrophilic block copolymers and additive controlled crystallization. He has published more than 390 papers and was listed among the top 100 chemists 2000 – 2010 worldwide by Thomson Reuters.

**How to cite this article:** Ni B, Cölfen H. Chirality communications between inorganic and organic compounds. *SmartMat*. 2021;2:17-32.  
<https://doi.org/10.1002/smm2.1021>